Artículo de Investigación / Research Manuscript

Revisión, observaciones y consideraciones sobre la erosión a alta temperatura en PS TBC para inspección técnica en turbinas a gas

High temperature erosion observations, considerations and overview in PS YSZ TBC for power gas turbine technical inspection

Augusto César Barrios[1], Gabriel Jaime Ovalle[2], José David Acosta[3], Andrés Felipe Sánchez[4], David Alejandro Marulanda[5], Óscar Alejandro Arroyave[6], Freddy Jiménez Navas[7], Carlos Mario Serna[8]

Fecha de recepción: 31 de mayo de 2013

Fecha de aceptación: 20 de julio de 2013

Resumen

La erosión es considerada como la segunda causa de falla en turbinas de generación y es un factor que limita el tiempo en operación de sus componentes. En el mantenimiento preventivo de estos equipos existen técnicas clásicas para determinar fallas en campo. Estas son: Inspección con boroscopio, con corrientes de Eddy y radiografías. Sin embargo,

Grupo de Tribología y Superficies, Universidad Nacional de Colombia sede Medellín

1 acbarriost@unal.edu.co

2 gjovallec@unal.edu.co

3 jodacostaco@unal.edu.co

4 afsanchezl@unal.edu.co

5 damarulandac@unal.edu.co

6 oaarroyaveg@unal.edu.co

7 jimen_nava@hotmail.com

8 cmsernaz@unal.edu.co

A. C. Barrios, G. J. Ovalle, J. D. Acosta, A. F. Sánchez, D. A. Marulanda, O. A. Arroyave, F. Jiménez, C. M. Serna "Revisión, observaciones y consideraciones sobre la erosión a alta temperatura en PSTBC para inspección técnica en turbinas a gas" Revista CINTEX, Vol. 18, pp. 297-324. 2013.

el reto consiste en correlacionar las microestructuras erosionadas de las barreras térmicas TBC con los modos de falla en los álabes de primera etapa y las cámaras de combustión. Este trabajo trata de aproximarse a los estudios científicos en erosión para tener criterios de evaluación en las inspecciones técnicas y en la predicción de la vida útil de los componentes. La primera parte consta de la caracterización de las superficies erosionadas del liner o combustor y los álabes de primera etapa obtenidos de una turbina GE7FA usada por EPM en la generación de energía. La segunda parte cubre la relación entre los hallazgos en la caracterización y la literatura, y reportes técnicos

PALABRAS CLAVE: Barreras Térmicas, erosión, álabe de turbina, inspección en turbinas, TGO, delaminación, TMF, CTE, coeficiente de expansión térmica

Abstract

Erosion is considered the second cause of failure in power gas turbine operation and it is a factor that limits the lifetime of turbine components. In corrective and preventive maintenance of these devices there are some classical techniques in order to determine failure in situ like Boroscopic inspection, Eddy Current testing and Radiography; however the challenge consists in correlating the erosion microstructure of Thermal Barrier coatings (TBC) with the failure modes in first stage turbine blades and combustion liners. This work tries to approach scientific studies on erosion to evaluation criteria in technical inspection and lifetime prediction of gas turbine components. The first part consists in the characterization of the liner and first stage turbine blades eroded-surfaces obtained from a Gas turbine GE7FA used by EPM for power generation. The last part states the relationship between characterization of the erosion and the literature and technical reports.

KEYWORDS: TBC, Erosion, Turbine blade, turbine inspection, TGO, Delamination, TMF, CTE.

1. Introduction

The plasma sprayed thermal barrier coatings of 7% yttria partially stabilized zirconia thermal barrier coating (YSZ PS-TBC) keeps the preponderance of the industry due to cost-reliability benefits for land-based turbines in power generation and other hot path devices and components [1-3].

Thermo-mechanical properties have been an important way in order to understand the YSZ PS-TBC operation performance. In this context, the high temperature erosion is considered the second factor that limits the lifetime of turbines and it increases its effect under high turbine entry temperatures TET [1-5]. The thermal cycling in non-standing operation turbines represents a great strain in turbine blades, thermal mismatch between the top coat (TC) and substrate, and then, the large stresses cause spontaneous failure on cooling [4,5]. For corrective and preventive maintenance, the visual inspection

during operation is considered primordial in order to determine the TC failure and sometimes, its mechanical behavior. Inspection techniques are the Colonoscopy Technique, Eddy Current inspection, High Temperature Revealing Ink, Luminescence Spectroscopy, X-ray Radiography and other techniques[6-9]. Although, the visual inspection of hot path turbine components gives some important information about the mechanical failure and response of the Top Coat (TC), the results should be correlated with the eroded structures. The erosion mechanisms of the PS-TBC can be identified by characterizing its splat morphology, flaws, pores, unmelted particles and oxides on the eroded surfaces. The mechanisms then can be correlated with the erosion conditions and thermo-mechanical load on the turbine. The challenge is to determine which of these factors lead to material removal and failure. It has been demonstrated that the TC removal in PS-TBCs occurs among the Top Coat and the Thermally Grown Oxide (TC-TGO) interfaces when bearing Thermomechanical Fatigue (TMF) [10]; especially when rumpling takes place, it specifically reduces the effective contact between TC and Bond Coat (BC)[11]. The high temperature erosion mechanisms and models are still being made; the classical elastic and elasto-plastic indentation concepts are a driving force in order to understand the PS-TBCs response under combustion gas impact[12]. The correlation between erosion models, the YSZ PS-TBC characterization and the real turbine worn surfaces represent an approximation method in order to assess the life time of turbine components[13-14]. Clearly, the complexity of TBCs systems in several environment behaviors and their correlation represent a challenge for the XXI century [5].

2. State of the art: Erosion of YSZ PS-TBC Hertzian Cracking

The erosion concepts and mechanisms were initially studied for ductile materials like soft metals[15-17], these concepts evolved in order to deal with the erosion of brittle materials and anisotropic ceramics. The elastic regime works well under quasi-static conditions: elastic blunt particles, stable low temperatures, slow velocities and the elastic response of the material. Hertzian contact mechanics describes the stresses distribution beneath the surface and, the Grifith theory describes the crack stress threshold, crack initiation and its growth in isotropic brittle materials [18]. First works on the erosion field adopted the Hertzian elastic contact in order to make single particle

impact erosion models. The stresses distribution $\sigma_1\sigma_2\sigma_3$ where σ_1 (tensile stress), σ_2 (intermediate compressive-tensile stress) and σ_3 (highly compressive stress) form a circle of contact, then these stresses develop a crack ring and finally, a cone crack when the applied load is increased. The erosion is then governed by cracks intersection until they come up to the surface [21].

3. Lateral-Median cracking

However, the erosion in turbine components such as first stage blades and liners are under high velocities and temperatures, the impacting solid particles have a sharp shape. The elastoplastic indentation models were developed in order to approach the brittle material response under non-quasistatic conditions; the material elastoplastic threshold explains in which way that material responses to dynamic indentation [19-20].

Lawn and Swain have described the kind of cracks that are developed in a brittle material and their sequence: the material is deformed plastically beneath and in the vicinities of a sharp indenter, around the irreversible deformation the lateral cracks are developed inside and parallel to the surface, and median cracks are developed downward to the surface. The lateral cracks eventually may intersect the surface [18-21]. This sequence consists in the following steps:

- Around the sharp indenter a plastic deformation occurs, its size is as large as the size of the indenter load. This means that the plastic regime depends on the applied load.
- Once the highest stress point (into the volume of irreversible deformation) reaches the critical values, the energy is released as a crack formation called median cracks. These cracks nucleate and propagate from this point toward the surface.
- When the indenter is unloaded the residual stresses accumulated in the material facilitate the lateral crack growth.
- In erosion, all the mentioned cracks intersect and interact with the surface and other cracks, and then material is removed from the surface.

4. Dynamic Erosion parameters

Evans [22] wrote an overview where he had demonstrated graphically the lawn's indentation sequence and introduced a model with KD "dynamic frac-

ture toughness" obtained in a previous Speronello's work [23] in machining of brittle ceramics. The KD concept could be strange if we consider that K1C is a quasistatic concept; it is more a dynamic parameter that changes with the impact velocity than fracture toughness itself. This means an approach to erosion models that includes dynamic response of the materials. Hertzian fracture strongly depends on fracture toughness KC and the radius of the indenter while elastoplastic fracture depends on indenter load, critical radius of the sharp indenter and material hardness. Both regimes can occur in high temperature erosion.

5. Erosion in polycrystalline high toughness and brittle ceramics

One of the first approaches to erosion mechanisms for polycrystalline ceramics, and surprisingly for PS-TBC was developed in the middle of 80's. The model was a relationship between kinetic energy of the particle impact and the microstructure geometry for polycrystalline alumina. The erosion mechanism assumes that the impact energy of the erosive particles is transferred to the target material and it is released across the grain boundaries of the ceramic [24-26]. The K1C was an interesting parameter included in the model as a material response under impacts. As a result of eroded microstructure observations, the pits formed during impacts have similar geometry and size of the removed grain. This could be similar to splat remotion from the TC surface, then, the kinetic energy would be transfered through the contact between two splats.

6. Erosion, manufacture and microstructure of TBC

Although models and mechanisms have been developed for brittle ceramics, PS-TBCs systems respond according to their own microstructure and morphology. In the 80's, erosion tests were performed in order to determine the erosion mechanisms in PS-TBCs, some tests were carried out at 1287°C using 27µm alumina particles, impacting at 244m/s and 15° impacting angle. The obtained erosion rates were correlated with the TC pore morphology and distribution, the pores were classified into laminar inter-splat pores and rounded discrete spherical pores across the splats [27]. Proposed wear mechanisms, figure 1:

- At low erosion rates, abrasion mechanisms occur; they are localized and can be identified for plowing and local furrows.
- At medium erosion rates, the particles cause cracks that are propagated until they remove a whole splat.
- At high erosion rates the particles penetrate the surface and tunnels are formed between pores and splats in order to remove a great amount of mass.

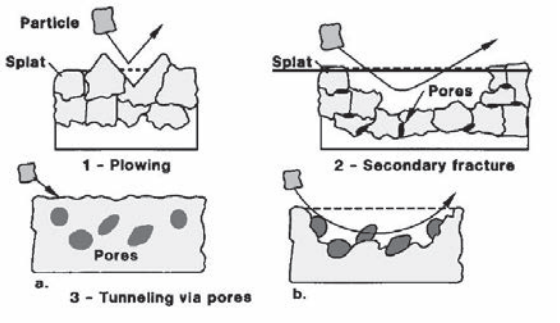

Figure 1. Graphic representation of three erosion mechanisms observed by eaton and novak in ps-tbcs (1) plowing; (2) secondary fracture; (3) tunneling via pores.

The type, the distribution and the concentration of pores can be correlated with the erosion rates and the material removal mechanisms and then this structure can be correlated with the plasma deposition processes, as a result, the erosion rates can be correlated with the manufacturing process of TBCs. At high deposition temperatures the erosion rates decrease because of the obtained microstructure, it has highly localized dispersed pores; other results on erosion rates exhibit changes in a factor of 2.5 between 15° to 90° impingement angle [27].

7. Effect of internal splat morphology in PS-TBCs

7.1 Erosion

Besides porosity and intersplat contact, the internal microstructure of the splat plays a role in the TC erosion mechanisms. The splat has a columnar structure with columnar cracks perpendicular to intersplat contact. These columns are formed during quenching, immediately after the plasma deposition [28]. The Figure 2 shows this internal splat microstructure. The splats

can be removed from surface in several steps under successive gas impact. The "columnar cracks" propagate across the splat forming intrasplat cracks, when a piece of cake of the splat is removed and the transplats cracks can be observed. A splat can be 1-4µm of thickness and 60µm of width.

There are three types of fractures observed in a splat structure: (i) Intrasplat: cracks formed across the splat only viewed on the surface. (ii) Intersplat: cracks formed between two splats from intersplat pores and (iii) Transplat: cracks formed across the splat and observed inside.

There was found that erosion mechanisms are governed by TC lamellar structure. Furthermore, the effect of PS-TBC's microstructure on erosion rates have had a strong effect on erosion rates; they have been correlated with "Mean bonding ratio", this concept is the quotient between lamellae and its thickness, and it expresses the bonding strength of splats. Under impacts the individual splats practically are spalled from the surface by crack propagation across the intersplat pores. It is found that erosion takes place in lamellar interfaces in TC and it depends on the splat thickness and contact size [30-31].

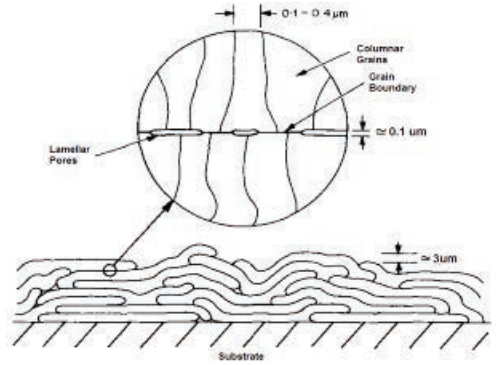

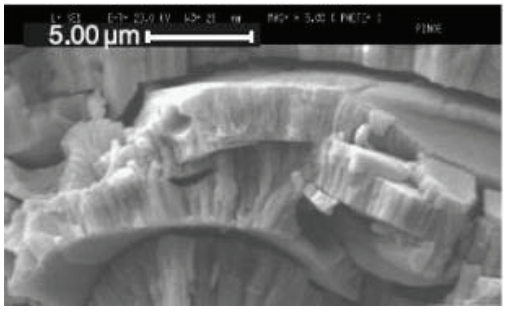

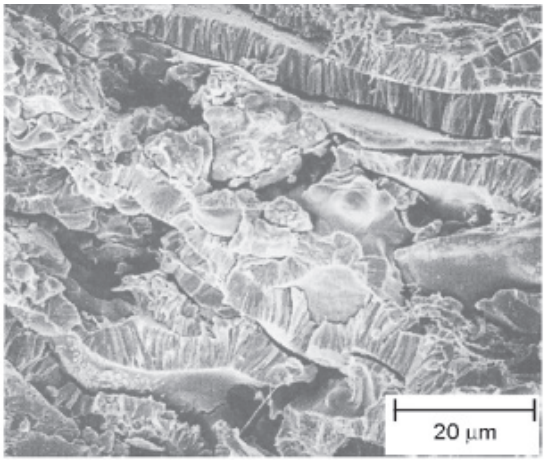

Figure 2. Morphology and columnar structure of splat [27-29].

8. Spalling and macroscale TC removal

The TC spalling is a combined phenomenon of ceramic thin layer removal, TGO growth and TMF. The erosion rates in this case are high because the volume and scale of mass loss in a complete piece of layer are greater than those of a single splat removal. The effect of both TGO growth and thermal mismatch on PS-TBC leads the TC decreasing properties and delamination. The great difference of substrate-TC coefficient of thermal expansion CTE in extreme operation conditions reveals a considerable amount of spalled TC layer [32-34].

9. Recent developments in TBC erosion

The erosion tests are trying to approach both, the TC porosity and the impact angle with the erosion rates [35]. The results, as expected, were: Porosity and angle of impact increase, as well as the erosion rates. The novel combination of techniques like AFM, DRX, SEM-EDS and the correlation of erosion variables could give some interesting results [35]. On the other hand, nano-indentation results on classical and modified PS-TBC will be a reliable parameter in erosion models and analysis [36].

10. Hot path components

10.1 Liner

In the liner starts the combustion stage, the hot gases impact at several angles, some of these are mainly parallel to the surface, as illustrated in Figure 3 a) and 3 b); there are three types of air in the combustion process: primary air ~15-20%, secondary air ~30% and tertiary air ~50-55%, figure 3 c). The turbine works with a considerable amount of air, usually in excess in order to complete the combustion process and avoid the high temperatures (due to flame in post-combustion) over the blades [33-38]. This excess of air generates an extra turbulence that may generate randomized erosion by gas impact and thermal degradation by localized high temperatures. The accumulation of carbon in the combustors generates the Foreign Object Damage (FOD) in the can walls and first stage blades.

10.2 First stage turbine blades

The complexity of the TC removal modes in a turbine blade require to accomplish a detailed study on erosive media. The eroding conditions include entropy generation: high energy dissipation cells, high frequency shock waves, and horse shoe paths [39-40]; see Figure 4. A foreign object damage FOD occurs when eventually, the contaminants are ingested into compression air, or particles are generated as a combustion sub-product (soot particles and other carbon solid structures) called domestic object damage DOD. Other event is the vibration transmitted from turbine rotor to blade, resonance contributes to substrate crack growth or high cycle fatigue HCF and subsequent TC removal [39-41].

The turbine blades receive all the products generated during combustion; some of these are contaminants that generate chemical attack. The localized heating in turbine blades as an entropy generation is difficult to control, under this condition, the creep appears combined with fatigue, thermal expansion mismatch (CTE differences between metal) and thermal aging. This cocktail of events elicits the TC loss in several ways. The TC loss and the resulting topographies are going to be analyzed in this article.

11. Reported Failure mechanisms in a turbine blade [40-44]

- Creep in hot sections (concavities and stagnation point)
- TMF (low cycle fatigue)
- HCF (high cycle fatigue): Generates cracking in substrate
- High temperature corrosion
- High temperature gas erosion
- High temperature oxidation
- FOD Foreign object damage and DOD Domestic object damage
- Delamination or spallation (Nucleation and propagation of cracks in TGO-TC interfaces)

12. Materials and methods

Hot path components (liner and first stage blades) of a gas turbine GE-7000FA were extracted in a preventive maintenance. The liner was sectioned using a Motortool as shown in pictures 5 and 6.

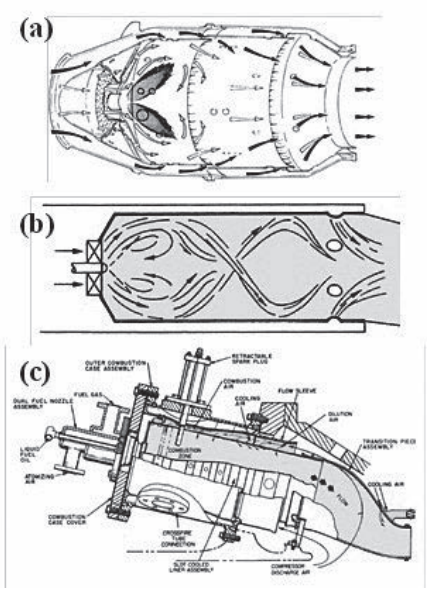

Figure 3. a) and b) gas flow patterns and impact zones on the liner´s wall, c) liner parts and devices [34, 37, 38].

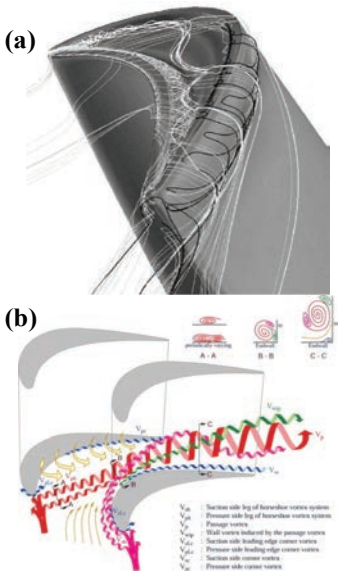

Figure 4. First stage turbine blade with (a) horse shoe path and (b) secondary flows [38].

The final cutting process for obtaining the test samples was performed using an Isomet® 5000 precision cutting machine at 4200 rpm and 1.2 mm/min feed-rate. These representative worn surfaces were selected in order to be characterized.

The first stage turbine blades were cleaned out and observed with a stereoscope on the suction and compression sides. Their characterized areas include stagnation point, tip, leading and trailing edge.

The standard porous PS-TBC samples with a four layer classical structure anatomy were analyzed: Inconel 625 substrate, MCrAlY bond coat (BC), 6-8%Y2O doped ZrO2 Top coat (TC) deposited by air plasma spray (APS) process and Thermal Growth Oxide (TGO). These new samples were compared with both worn liner and blade surfaces.

The sample surfaces were observed using stereo microscopy Nikon SMZ 1500. A scanning electron microscopy SEM Jeol 5910 LV was used to take the TC superficial and transversal images. The micrographs were processed and analyzed with NIKON NIS Elements in order to identify particles, degradation of the splats, fractures and erosion mechanisms on worn surfaces. For transversal characterization of eroded TC, the samples were embedded in resin: the metallographic preparation was performed by grinding the samples on

400 and 600 emery papers during five minutes followed by polishing clothes Ultrapath®, Texmet®, and Microcloth® with polycristaline diamond abrasive suspension of 12 μm, 6 μm, 3 μm and 1 μm, the final polishing was performed with 0.06 μm Silica suspension.

12.1 Measurement methodology, microstructural characterization

Superficial characterization of worn TC was performed. Initially the liner and eroded blade surfaces were observed with Stereo Microscopy in order to identify and select the most representative worn areas, the criteria was the topography changes in the splats observed in the inspection. A scanning electron microscopy (SEM) Jeol 5910 LV was used to take the TC surface and transversal images. An Energy Dispersive X-ray Spectroscopy (EDXS) detector was used at 15-25 KV acceleration voltage in order to perform chemical microanalysis on eroded areas. EDXS compositional maps were developed to identify the elements present on eroded surfaces.

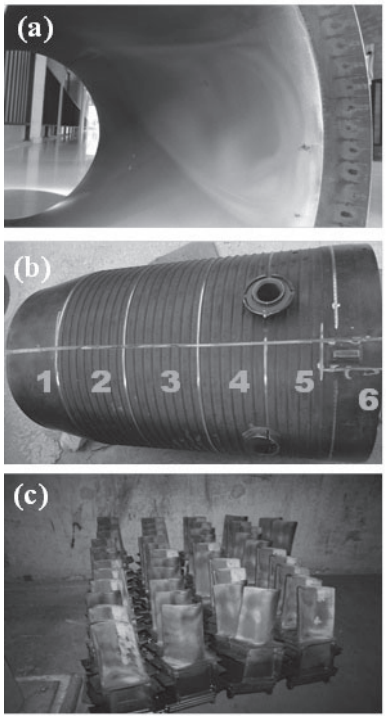

Figure 5. (a) And (b) Liner sectioning: the worn surfaces of the liner were identified and classified. (c) Gas turbine blades extracted during maintenance. Courtesy EPM.

13. Turbine combustion chamber: Liner

In several areas of the liner the rounded particles are found, the EDS results confirm that their composition is mainly YSZ. The other composition amounts correspond to contaminants like Ca and Fe, the foreign objects in the environment and main composition of revealing ink, respectively. It is possible that unmelted YSZ particles were deposited at lower temperatures than formed splats in the plasma spray process. The statistical results on unmelted particles show values between 20 to 264 µm of diameter with a mean of 110 um.

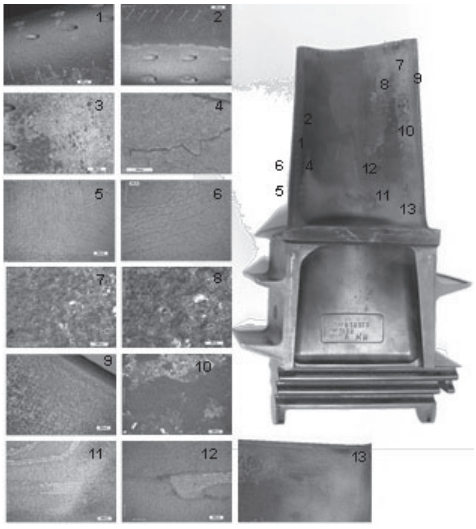

Figure 6. Liner dissection, several topographies were obtained by stereoscopy across the gas flow path.

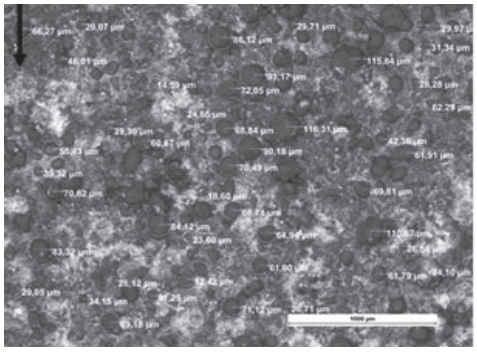

Figure 7. Measurements on eroded surface liner section 2D

Typical morphology of liner TC that include splats, unmelted particles and contaminants; The quality of a TC is defined by the level of splat formed during process. Figure a) in the plasma deposition process unmelted particles can cohere to form a single and larger particle, figure 8 b), this could determine other degradation mechanisms. In figure 9 the transition from major (left) to minor (right) erosion was observed, the gas flow moves and impact in certain zones according to the combustor position and combustion conditions, the secondary air also has effects on the flow direction of gas. The splat removal is more intense on the left side of this micrograph; the formed valleys may increase the roughness and gas turbulence near the surface.

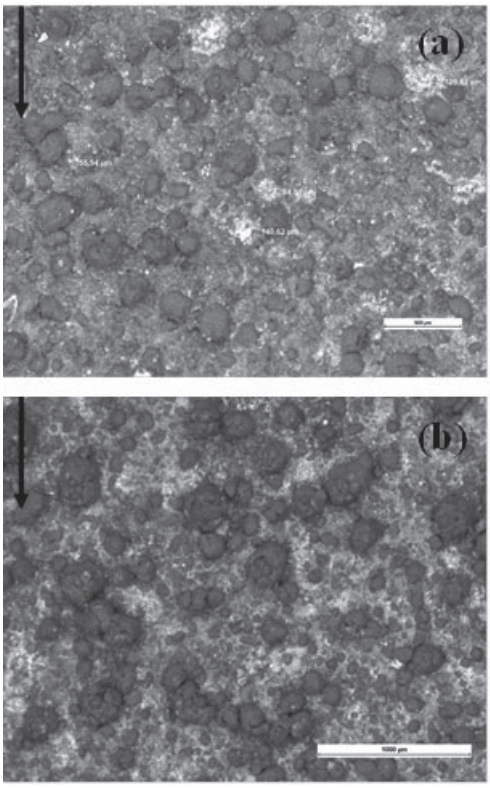

Figure 8. Stereoscopy micrograph of liner level 2 (a) detachment of unmelted particles and (b) their morphology. The black arrow indicates the average flow direction.

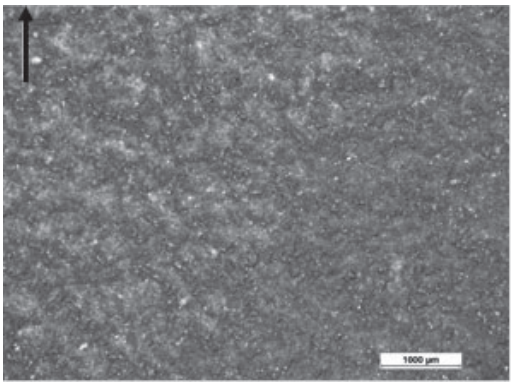

Figure 9. Stereoscopy micrograph of liner, section 3, center.

The great quantity of detached particles reveals a new TC surface again, the EDS test confirm that the new surface is TC and not BC. The size of the footprints may offer a perspective of the removed particles; the first removed ones are the larger particles. There is a tendency, the small unmelted particles have not yet been detached from the surface and the big ones leave a mark on the surface. These marks have a "halo pattern" due possibly to intersplat contact and noncontact area, Figure 10.

The surfaces far from the combustor show a mild erosion, the primary stages of erosion discover and expose the unmelted particles via splat removal. In these cases, the splats on top of these particles were detached at first, figure 11.

The zones where the splats are well deposited present a uniform pattern of wear with defined intersplat spaces and limits. The splat structures are degraded possibly because of high localized temperatures. By contrast, in figure b) there is a great quantity of unmelted particles in a wide size distribution. In the erosion process there are two possibilities: the particles appear after splat removal or the particles were removed first, the first event is not defined yet, but the micrograph b) may offer a tendency: the red ink on valleys means splats were not removed at first.

EDS results reveal that the composition in the valleys was mainly Zr as expected but in the peaks of the splats appear Ca and Fe as contaminants. In Figure 14 the Ca contaminants appear as scattered dots.

14. Eroded first stage turbine blade

Worn First stage turbine blade, the picture 15 shows different zones and their erosion level, compression side, stagnation point and tip of the blade suffer the major erosion. Visual inspection reveals preferential erosion points due to the combination between thermo-mechanical fatigue or TMF and the combustion gas impact. On the trailing edge both can be appreciated, spallation and gradual erosion of BC y TC. The TC loss in these points leads to the end of the blade lifetime and power losses.

In some areas of the compression side the gradual erosion and TC mass loss take place; although this erosion occurs preferentially, the possible cause is a gas impacting randomly on the blade surface. Figure 15 reveals this phenomenon, the TC is the brown-orange darker surface, this color is due to the high temperature revealer ink and corrosion; the BC shows cream surface and the gray and deeper one is the substrate.

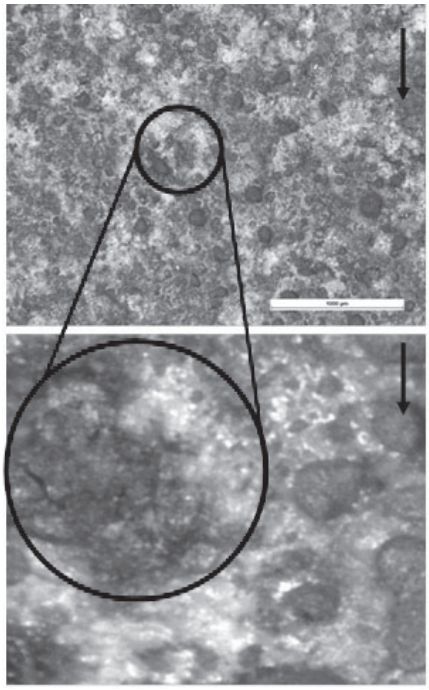

Figure 10. Stereo micrograph of tc of liner 2d, there is a wide particle removal across de surface; the imprint morphology indicates the intersplat or splat/particle contact area.

TC degradation by spallation: 1. Delamination or spallation; 2. Exposed perpendicular TC microstructure under gas impact leads to a second spallation. In the Figure 18, the localized spallation occurs in the high temperature zone that allows the crack nucleation in thermal mismatch. The thermal mismatch is intensified by nominal operation conditions as periodic or cyclic operation and their thermal gradients like EPM combined cycle power plant. The spallation follows a linear pattern that continues across the length of the blade, it can be explained for the section changes in the concavity, this means high temperature profiles and abrupt changes in their thermal gradients.

In the trailing edge the combination between spallation and gradual TC erosion make the worn morphology. This zone is characterized for shockwaves impact and high energy rotational cells caused by boundary layer loss. Some qualitative changes in surface roughness are observed in Figure 19, this could generates more erosion and power loss due to rotational cells. Although the erosion patterns reveal gradual mass loss, they are considerable compared with other surface areas in the blade, the mechanisms do not include an abrupt mass loss or marked spallation, the mass loss come from the surface. In some areas the BC appears with some points where substrate is arising.

Radial cracks in the center of the compression side developed perpendicular to blade hub and others have an inflection to trailing edge in their propagation. These cracks facilitate material removal; a weak fatigued TC is more susceptible to failure under gas impacts, the TC is delaminated besides the cracks, figure 19. In this case the crack growth appears within erosion and in this condition is difficult to determine which event occurs at first. The roughness was increased possibly by splat removal, Figure 20.

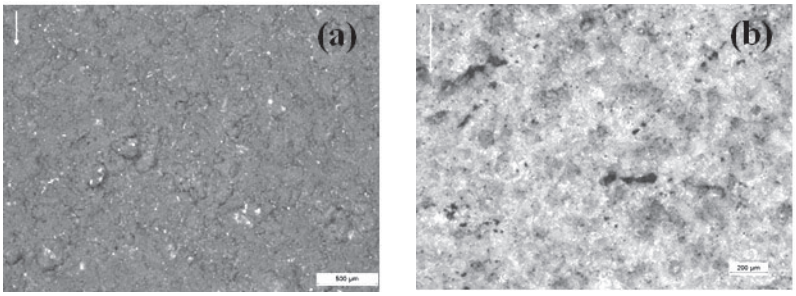

Figure 11. Two sections of the liner, far from the combustor, (a) the first micrograph has revealing ink and (b) the appearance of the tbc when deposited.

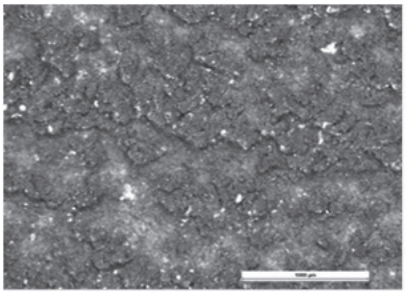

Figure 12. Well deposited splats, thermally degraded and some other were removed.

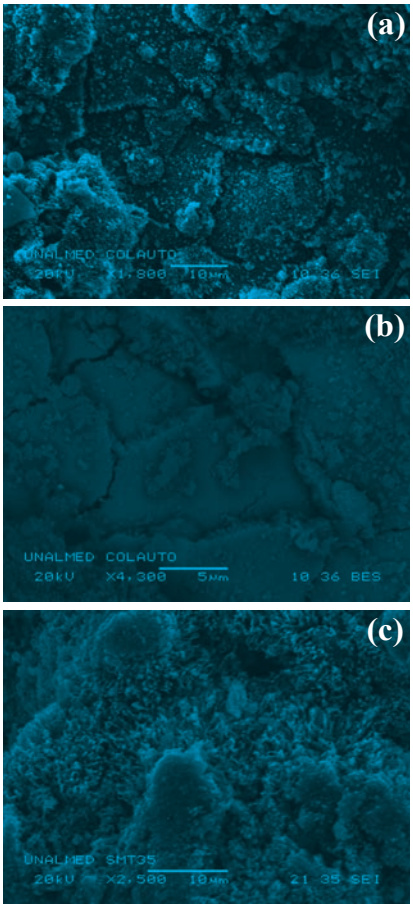

Figure 13. Three types of degradation: (a) (b) splats are removed by parts via intra splat cracks, (c) internal columnar structure revealed by erosion

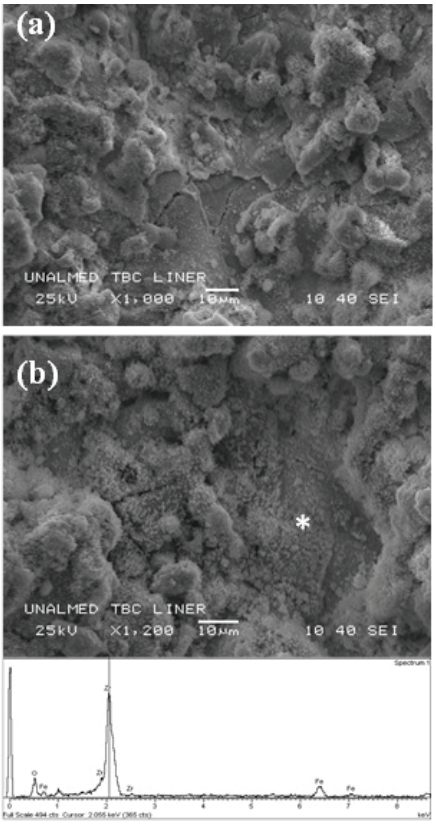

Figure 14. Sem micrograph of liner surface with three types of splat cracks

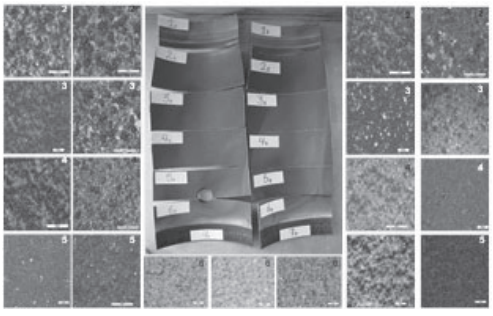

Figure 15. Turbine first stage blades. 1, 2 And 4: trailing edge and stagnation point. 3, 7, 8, 9 And 10: leading edge near the tip, compression side. 5 And 6: suction side. 11 And 12: compression side, high temperature surface and 13: base of the blade

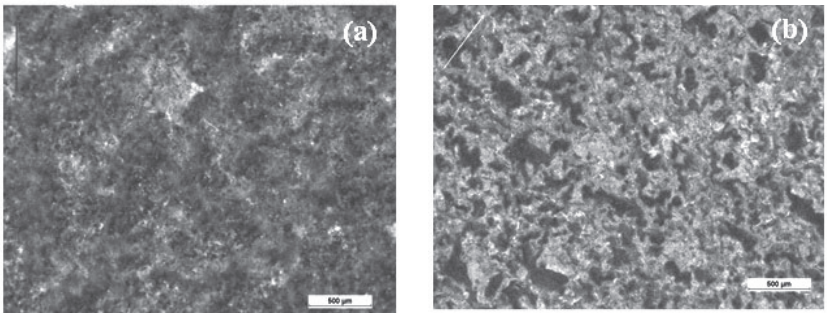

Figure 16. Stereo micrographs of compression side with serious but gradual erosion by splat removal.

The aerodynamics holes in the leading edge have cracks possibly caused by thin substrate thickness near the surface Figure 21 (a). These kind of cracks start in the hottest section of the blade, their length can reach the 2 mm. Around the stagnation point the thermal degradation combined with the erosion facilitate the TC delamination and its removal, this can be explained by high thermal gradients generated from the temperature difference between cooled substrate and TC surface, Figure 21 (b).

The cracks in the suction side grow transversely near the leading edge and they grow longitudinally near the middle of the surface, intersecting both at the central zone while the cracks in the compression side, especially in the high temperature zone grow longitudinally. At high speed in the turbines (3600 rpm) the centrifugal forces generate axial cracks like those observed in Figure 22.

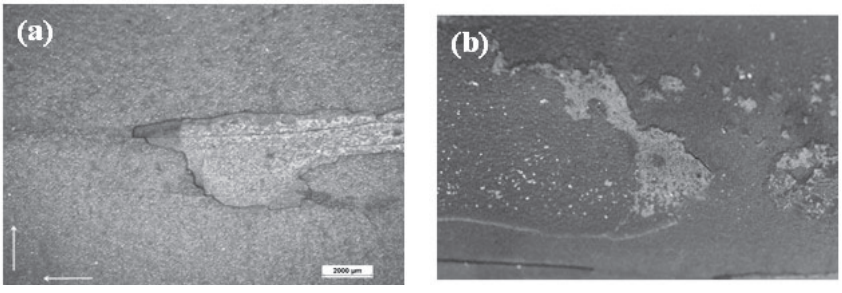

Figure 17. (a) stereoscopy of a delaminated tc in compression side (b) photography of tc delaminated by steps in compression side.

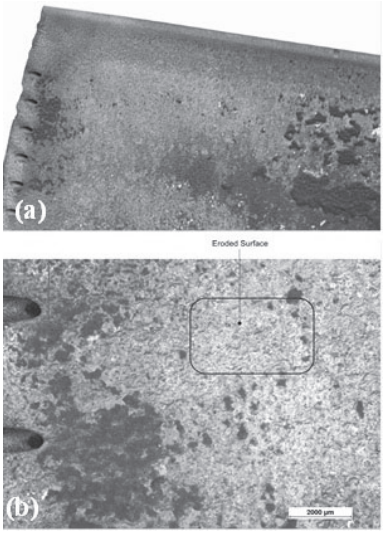

Figure 18. Near the tip the erosion is gradual, left. In the center of the blade at the trailing edge the spallation governs the tc removal, right.

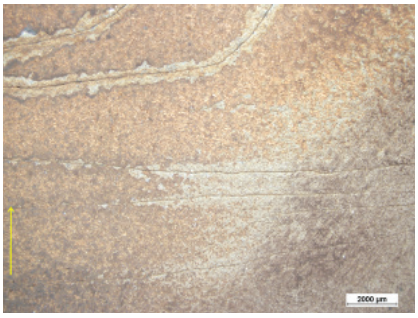

Figure 19. Radial cracks into compression side.

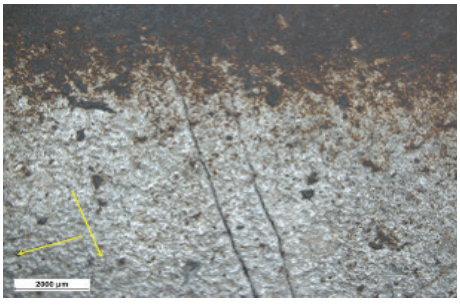

Figure 20. Combined transversal cracks and high temperature erosion by splat removal.

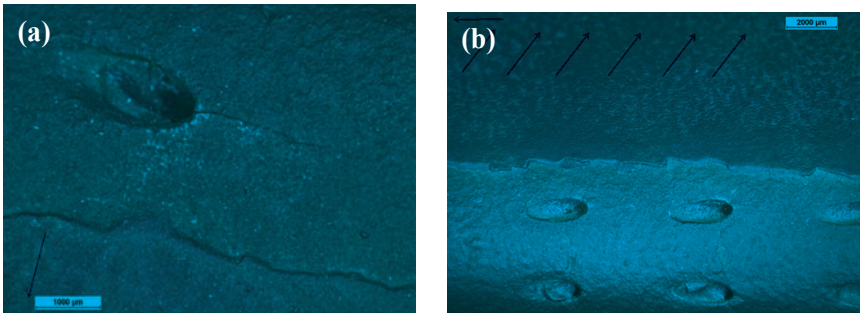

Figure 20. (a) and (b) micrographics of trailing edge with spallation or delamination by tmf and erosion.

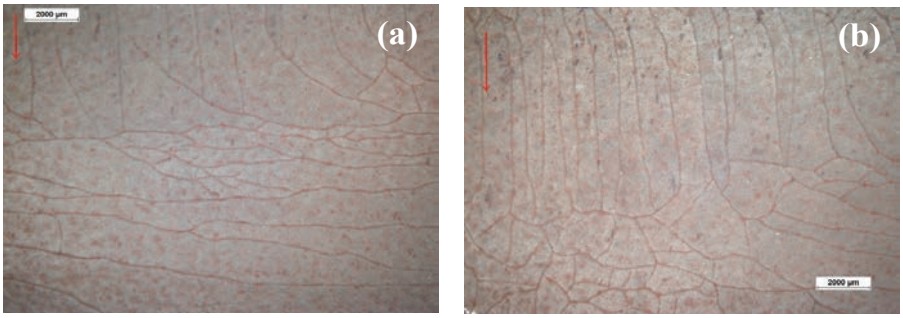

Figure 22. Tc radial and transversal cracks patterns in the middle of the suction side; the arrows indicate the gas flow direction.

15. Discussion and concluding remarks

15.1 Liner

Major erosion is observed on surfaces located under path flow, in these areas the TC was soaked by the impact of the combustion gases more frequently than other liner areas. Previous works have established that impact kinetic energy is proportional to wear rates, although these rates stabilize near at 1000°C [26]. This assumption could apply in liner but not in turbine blades.

The kinetic energy decreased across the liner from combustor to liner/transition piece coupling, the restriction to flow reduce the velocity of the gas; it may be a reason why the surfaces far from the combustor were no significatively eroded. The new surfaces like valleys where splats/particles

were removed facilitate gas turbulences; these rotational cells can protect or erode the other splats.

Due to the combustors position many gas impact angles are less than 90° but the angle effect in a restricted flow was no determined by micrographs. Other interesting findings were the crack propagation from a pore, previous works [26-27] indicate the proportional relation between pore concentration and erosion rates.

The greater size unmelted particles are more susceptible of being detached because they generate more opposition to the flow. Although the remotion depends on the flow direction and intensity, the big unmelted particles are removed at first. The areas impacted directly by combustion gases present high erosion levels as expected; other surfaces reflect thermal degradation due to direct contact with flame in the main path flow.

The first detachment of splat or unmelted particles is undefined but the mechanisms reflect a TC erosion via intersplat crack propagation according to literature [26-31]; the new surface is generated as valleys that increase roughness and then gas turbulences near the surface.

Although the relationship between gas impact and material fracture has been recently developed and no matter how difficult it can be, there is a clear evidence that it alone promotes TC fractures and removal in collaboration with eventual FOD or DOD.

There are no evidence of plows, furrows or channels in TC surfaces. The observed mechanisms are TMF (randomly crack propagation) and thermal degradation.

According to literature the kinetic energy of the impact body (or gas) is totally transferred to the intersplat limits leading to the splat/particle removal, but SEM micrographs indicate a kinetic energy that was released to trans-intrasplats cracks and discrete pores gradually eroding the splats as defined in other works [31]. The splat surface is degraded to reveal its columnar structure. Many erosion models are based on impacts of an elastic body with defined indentation geometry, under these limited possibilities the worn surfaces just were classified in mild, medium and strong erosion.

The unmelted particles may be more susceptible to erosion than splats due to the contact area in the splats is greater than the particles. Even when

the splats are removed by parts like a piece of cake due to intra and transplats crack propagation and effective contact area. It could be assumed that the unmelted particles or splats not always are completely detached from the surface.

In general, the erosion patterns in the liner decrease, according to the analyzed surface this decrese is farther from the combustor.

16. Turbine Blades

The high temperature zone was affected by thermal mismatch and TGO growth causing clearly a TC spallation; the next step is the BC thermal degradation and erosion. Although TGO is not observed; it appears immediately after plasma spray deposition of YSZ, and continues its growth until 7 or 8 μm where the TC spallation occurs [32-33]. The TC remotion on the trailing edge was carried out at high rates compared with the suction side and the base of the blade. The erosion was accentuated by shockwaves.

The TGO growth plays an important role in the blade erosion; it contributes along with TMF to spallation. The differences between substrate, BC, TGO and TC coefficient of thermal expansion CTE under high loading operation at full speed of the turbine lead to the crack formation and subsequent material loss beneath the shock waves impact. Other blade zones present progressive mass loss via splat removal and roughness generation; some causes are reported in literature, shock waves, random hot gas impact and rotating cells.

According to literature, axial cracks are formed under axial forces at high rotational speed; transversal (radial) cracks are formed due to a temperature gradient between leading edge and trailing edge. The observed cracks were developed in the compression and the suction side of the blade. They could be intersected with lateral and median internal cracks removing the TC and contributing to erosion. The hole's crack in the blade leading edge can be attributed to the TC loss by TMF and the thermal mismatch in a thin substrate layer. The damage can continue affecting the aerodynamic of the blade causing power loss.

Although it is not observed, TGO growth plays an important role in the blade erosion; it contributes along with TMF to spallation. The differences

between substrate, BC, TGO and TC coefficient of thermal expansion CTE under high loading operation at full speed of the turbine lead to the crack formation and subsequent material loss beneath the shock waves impact.

The erosion near the tip is affected by the turbulence and the high energy dissipation cells like horseshoe path. Experimental results for blade and the coating material erosion indicate that erosion surface roughness increases with the eroding media impact velocities and impingement angles and those eventually larger particles produce higher surface roughness according to previous works [45]. Stagnation point, delamination by TMF combined with erosion.

17. Acknowledgments

Thanks to EPM, Colciencias and GTS UNAL. Thanks to Alejandro Toro Betancur and Pablo Gómez Flórez for their support.

18. References

[1] D. R Clarke, and C. G. Levi. "Materials design for the next generation thermal barrier coatings". Annual Review of Materials Research 33.1, 383-417. 2003.

[2] J. R. Nicholls, M. J. Deakin and D. S. Rickerby. "A comparison between the erosion behavior of thermal spray and electron beam physical vapor deposition thermal barrier coatings". Wear 233–235; 1999.

[3] S. M. Meier, D. K. Gupta. "The evolution of thermal barrier coatings in gas turbines engine applications". Journal of Engineering for Gas Turbines and Power 116, 1994.

[4] R. G. Wellman, J. R. Nicholls and K. Murphy. "Effect of microstructure and temperature on the erosion rates and mechanisms of modified EB PVD TBCs", Wear 267; 2009.

[5] N. P. Padture, M. Gell and E. H. Jordan. "Thermal Barrier Coatings for Gas-Turbine Engine Applications". Review: Materials Science, Science's Compass Vol. 296, 280; 2002.

[6] D. Balevic, S. Hartman and R. Youmans. "Heavy-Duty Gas Turbine Operating and Maintenance Considerations". GE Energy, GER-3620L.1, 2010.

[7] D. G. Robertson, C. Zhou. "Power, Petrochemical/ Refining and Process Plant: Survey of Advanced Inspection Techniques & Recommendations for Best Practices". European Technology Development Limited, ETD Report No: 1077-gsp-72; 2008.

[8] Technical Data, Brouchure, GE Sensing & Inspection Technologies, "Productivity through inspection solutions Inspection Technologies"; 2009.

[9] Brouchure GE Sensing & Inspection Technologies; "Corrosion & Erosion: Inspection solutions for detection, sizing & monitoring"; 2010.

[10] E. Tzimas *et al*. "Damage and Failure Mechanisms of Thermal Barrier Coatings under Thermomechanical Fatigue Loadings". Thermomechanical Fatigue Behavior of Materials: 4th Volume, ASTM STP 1428, 2003.

[11] V. K. Tolpygo, D. R. Clarke. "Rumpling induced by thermal cycling of an overlay coating: the effect of coating thickness". Acta Materalia, 2003.

[12] R. G. Wellman, J. R. Nicholls. "High temperature erosion–oxidation mechanisms, maps and models"; Wear 256, 2004.

[13] A. Hamed and W. Tabakoff. "Erosion and deposition in Turbomachinery". Journal of Propulsion and Power", Vol. 22, No. 2, March–April 2006.

[14] W. Tabakoff, A. Hamed and V. Shanov. "Blade deterioration in a gas turbine engine". International Journal of Rotating Machinery, 1998.

[15] I. Finnie. "Erosion of surfaces by solid particles"; wear 3, 1960.

[16] J. G. A. Bitter. "A study of erosion phenomena part I, part II", Wear 6, 1962.

[17] G. Grant, W. Tabakoff. "An experimental investigation of the erosive characteristics of 2024 aluminum alloy". National technical Information Services, U.S. Army Research Office-Durham, 1973.

[18] B. R. Lawn; F.C. Frank, F. R. S. "On the theory of Hertzian fracture". Ed. Proceedings of the Royal Society, 1967.

[19] B. R. Lawn, M. V. Swain, "Microfracture beneath point indentations in brittle solids". Journal of Material Science, 1975.

[20] B. R. Lawn, Equilibrium penny like cracks in indentation fracture, 1975.

[21] B. R. Lawn, A. G. Evans and D. B. Marshall. "Elastoplastic damage in ceramics: The median/radial crack system". The American Ceramic Society, 1980.

[22] A. G. Evans, T. R. Wilshaw. "Quasistatic solid particle damage in brittle solids I. Observations, analysis and Implications", Acta Metallurgica 24.10, 939-956, 1976.

[23] R. W., Rice, B. K., Speronello. "Effect of microstructure on rate of machining of ceramics". American ceramic Society, 1976.

[24] J. E., Ritter, *et al*. "Erosion Damage in Glass and Alumina". The American Ceramic Society, 1984.

[25] E. Ritter. "Erosion damage in structural ceramics". Materials Science and Engineering, Vol. 71, 1985.

[26] J. E. Ritter, L. Rosenfeld and K. Jakus. "Erosion and strength degradation in alumina". Wear, vol.111; 1986.

[27] H. E., Eaton and R. C., Novak. "Particulate erosion of plasma sprayed porous ceramic". Surface and Coatings Technology, Vol. 30, 1987.

[28] A. Portinha. "Characterization of thermal barrier coating with a gradient in porosity", Surf. Coat. Tech, 2005.

[29] Handbook of Thermal Spray Technology. Handbook; ASM International; 2004.

[30] R. Mc Pherson. "A review of microstructure and properties of plasma sprayed ceramic coatings". Surface and Coatings Technology, 39-40; 1989.

[31] C. J. Li, G. J. Yang and A. Ohmori. "Relationship between particle erosion and lamellar microstructure for plasma-sprayed alumina coatings"; Wear, 2006.

[32] A. G. Evans *et al.* "Mechanisms controlling the durability of thermal barrier coatings"; progress in materials Science; 2001.

[33] J. R. Nicholls, M. J. Deakin, D. S. Rickerby. "A comparison between the erosion behavior of PS and EBPVD TBC". Wear, 1999.

[34] A. Rabiei, A. G. Evans. "Failure mechanisms associated with the thermally grown oxide in plasma-sprayed thermal barrier coatings". Acta Materalia Vol. 48; 2000.

[35] C. S. Ramachandran, V. Balasubramanian and P. V. Ananthapadmanabhan. "Erosion of atmospheric plasma sprayed rare earth oxide coatings under air suspended corundum particles". Ceramics International, 2013.

[36] Y. Wang *et al*. "Microstructure and indentation mechanical properties of plasma sprayed nano-bimodal and conventional ZrO2-8wt%Y2O3 thermal barrier coatings"; Vacuum Vol. 86; 2013.

[37] P. K. Wright, A. G. Evans, "Mechanisms governing the performance of thermal barrier coatings". Current Opinion in Solid State and Materials Science, Vol. 4; 1999.

[38] M. P. Boyce. Gas Turbine engineering handbook, Second Edition; Ed. 2002.

[39] A. Giampaolo. "Gas Turbine Handbook: Principles and Practice". Ed. The Fairmont Press, Inc. 2009.

[40] M. Papa, R. J. Goldstein, F. Gori. "Numerical heat transfer predictions and mass/heat transfer measurements in a linear turbine cascade". Applied Thermal Engineering; 2007.

[41] C. B. Meher Homji and G. Gabriles. "Gas turbine blade failures, causes, avoidance, and troubleshooting"; ATM, Proceeding of the 27th Turbomachinery Sympossium.

[42] Z. Mazur, A. Luna-Ramírez, J. A. Juárez-Islas, A. Campos-Amezcua. "Failure analysis of a gas turbine blade made of Inconel 738LC alloy", Engineering Failure Analysis 2005

[43] R. C. Reed. The superalloys, fundamentals and applications. Cambrige press 2006. p. 324.

[44] B. Baufeld, M. Bartsch, S. Dalkilic, M. Heinzelmann. "Defect evolution in thermal barrier coating systems under multi-axial thermomechanical loading". Surfaces and coatings technology; 2005.

[45] A. H. Atwater, W. Tabaco. "F Turbine Blade Surface Deterioration by Erosion". ASME Journal of Turbomachinery, Vol. 127, 2005.